Available online at www.sciencedirect.com
SCIENCE DIRECT®
Journal of Sound and Vibration 272 (2004) 607–625
JOURNAL OF SOUND AND VIBRATION
www.elsevier.com/locate/jsvi

Multi-dimensional vibration power flow analysis of compressor system mounted in outdoor unit of an air conditioner

Ho-Jung Lee, Kwang-Joon Kim*

Department of Mechanical Engineering, Center for Noise and Vibration Control, KAIST, Science Town, Daejeon 305-701, South Korea

Received 20 July 2002; accepted 27 March 2003

Abstract

Vibration generated by an excitation source is in general transmitted to a receiver structure through multiple paths, i.e., multiple points in multiple directions. The multi-dimensional vibration transmission path analysis can be effectively accomplished by employing the vibration power approach because the contribution of each path to the total vibration transmission can be readily represented and, furthermore, the vibration power transmitted to the receiver is closely related to the noise radiation from the receiver. The main content of the work presented in this paper is to apply the concept of the vibration power flow to a practical system of multi-dimensional vibration isolation systems for the vibration transmission path analysis. In addition, the role of the vibration power flow will be illustrated as a measure of the vibration transmission onto as well as the resultant noise radiation from the receiver structure.

In this paper, the vibration power flow approach is applied to a compressor system mounted in outdoor unit of an air conditioner in order to determine the most dominant transmission path. Then, the frequency characteristics of the vibration power flow to the receiver structure are compared with those of the structural vibration level on and the resultant noise emission from the receiver structure.

1. Introduction

In a practical vibration isolation system, vibration is transmitted from a source to a receiver through several paths, i.e., at more than one inter-connected point and with multi (translational and rotational) degree of freedom at each point. With increase of complexity in such an isolation

*Corresponding author. Tel.: +82-42-869-3024; fax: +82-42-869-8220.
E-mail address: kjkim@mail.kaist.ac.kr (K.-J. Kim).

0022-460X/03/$ - see front matter
doi:10.1016/S0022-460X(03)00386-9

system, more efficient vibration transmission path analysis techniques are required. The method of vibration power flow is a good solution for this purpose. The reason for this is that the vibration power transmission through each path can be easily represented by a ratio to the total vibration power transmission and, furthermore, the vibration power transmitted to the receiver structure is considered to be closely linked to the noise radiation from the structure.

Although, however, mathematical formulations for the vibration power estimations have almost been completed by many researchers, their applications to practical systems still encounter difficulties mainly due to instrumental limitations especially in rotational motions. Therefore, in most literatures, investigations have been done mainly by the numerical analyses or at the best experimental studies on simple beam/plate-like structures. Experimental results for practical systems with the rotational terms included have been reported rarely. In addition, although the effectiveness of the vibration power in the prediction of the noise radiation from the receiver has been mentioned often in literatures, the experimental comparison of the vibration power flow to the receiver with the noise radiation from it has never been shown even from the qualitative aspects.

Moorhouse and Gibbs [1] estimated the vibration power transmission for resiliently mounted compressors by employing the mount dynamic stiffness and the accelerations on the top and the bottom of the mount, but the vibration power was assumed to have a vertical component only. They thereafter measured the rotational components for machines on floor by transfer mobilities between excitation points and arbitrary points on the supporting structure and then claimed that the moment becomes important even at low frequencies when the vibratory source is located near an edge of the receiver structures [2].

Koh and White [3,4] were concerned with the vibration power transmission onto a beam- or plate-like supporting structure at a single connection point subject to simultaneously acting sinusoidal force and moment excitations. They showed from the experimental results that the coupling mobility between the translational and the rotational terms can give rise to some cancellation of the vibration power and illustrated that the vibration power can be minimized by adjusting the moment excitation.

There are some researchers who employed the vibration power as a cost function for active vibration isolation. Gardonio et al. [5,6] measured and predicted the structural vibration transmission between two plates, which are mechanically coupled by an active mount. Howard et al. [7] took a flexible beam structure as the receiver of an experimental model for the same purpose. However, they took the rectilinear motion solely at mounts into consideration in the vibration power approximation.

Significance of the rotational motions at inter-connected points between sub-structures has been investigated by the numerical analyses only. A recent research by Sanderson [8] showed that both over- and under-estimation of the vibration power transmission can be significant especially in the high-frequency range when rotational stiffness of the isolator is not taken into account. Lee and Kim [9] showed the effects of the rotational terms by the decomposition of the total vibration power into the vibration power transmissions related to pure translational motions, pure rotational motions and coupling between translational and rotational motions and they also investigated the relations of the erroneous peaks in the vibration power approximations to dynamic characteristics of the underlying system.

In this paper, the concept of the vibration power flow will be applied to a compressor system mounted in the outdoor unit of air conditioner for the vibration transmission path

analysis. In addition, the effects of exclusion of the rotational terms at each path in the vibration power transmission will be demonstrated. The vibration power transmission with the rotational terms considered will be compared with the noise emission from, and the structural vibration level on, the surfaces of the compressor system. Furthermore, similar analysis results will be discussed for the same system in which one of the vibration transmission paths is isolated.

2. Theory of power flow in multi-dimensional vibration isolation system

Let us first consider a multi-point vibration isolation system as shown schematically in Fig. 1, where a source with m excitation forces is connected to a receiver at n points. When six (three translational and three rotational) degrees of freedom (d.o.f.) are considered at each of the n connection points, the total vibration power input to the receiver is given by

$$\begin{aligned} P_R &= \tfrac{1}{2}\mathrm{Re}\{\mathbf{F}_R^*(\omega)\mathbf{V}_R(\omega)\} \\ &= \tfrac{1}{2}\mathrm{Re}\{\mathbf{V}_R^*(\omega)\mathbf{F}_R(\omega)\}, \end{aligned} \tag{1}$$

where $\mathbf{F}_R$ and $\mathbf{V}_R$ are, respectively, the $(6n \times 1)$ force and velocity vectors at the connection points on the receiver and the subscript and superscript, R and *, respectively, represent the receiver structure and conjugate transpose.

The receiver structure can be characterized dynamically by a $(6n \times 6n)$ mobility matrix $\mathbf{Y}_R$ or impedance matrix $\mathbf{Z}_R$ as follows:

$$\begin{aligned} \mathbf{V}_R &= \mathbf{Y}_R\mathbf{F}_R, \\ \mathbf{F}_R &= \mathbf{Z}_R\mathbf{V}_R. \end{aligned} \tag{2}$$

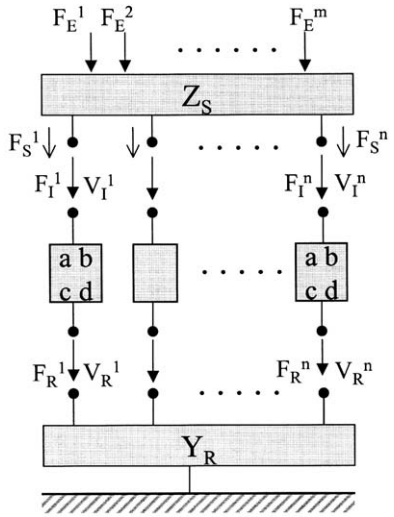

Fig. 1. Schematic representation of a multi-point vibration isolation system.

Then the vibration power flow to the receiver can be represented in various forms as follows using either the receiver mobility($\mathbf{Y}_R$) or the impedance($\mathbf{Z}_R$) matrix:

$$\begin{aligned} P_R(\omega) &= \tfrac{1}{2}\mathrm{Re}\{\mathbf{F}_R^*(\omega)\mathbf{Y}_R(\omega)\mathbf{F}_R(\omega)\} \\ &= \tfrac{1}{2}\mathrm{Re}\{\mathbf{F}_R^*(\omega)\mathbf{Y}_R^*(\omega)\mathbf{F}_R(\omega)\} \\ &= \tfrac{1}{2}\mathrm{Re}\{\mathbf{V}_R^*(\omega)\mathbf{Z}_R^*(\omega)\mathbf{V}_R(\omega)\} \\ &= \tfrac{1}{2}\mathrm{Re}\{\mathbf{V}_R^*(\omega)\mathbf{Z}_R(\omega)\mathbf{V}_R(\omega)\}. \end{aligned} \tag{3a–d}$$

As mentioned above, when six (three translational and three rotational) d.o.f.'s are considered at each of the n connection points, $\mathbf{F}_R$ and $\mathbf{V}_R$ are $6n \times 1$ vectors and $\mathbf{Y}_R$ and $\mathbf{Z}_R$, $6n \times 6n$ matrices, and the vibration power is transmitted to the receiver through $6n$ paths. The total vibration power transmission to the receiver given in Eq. (1) can be rewritten by the sum of the vibration power transmission through each path as follows:

$$\begin{aligned} P_R(\omega) &= \sum_{i=1}^{6n} P_i(\omega) = \sum_{i=1}^{6n} \frac{1}{2}\mathrm{Re}\{\bar{F}_i(\omega)V_i(\omega)\} \\ &= \sum_{i=1}^{6n} \frac{1}{2}\mathrm{Re}\{\bar{V}_i(\omega)F_i(\omega)\}, \end{aligned} \tag{4}$$

where $\bar{F}$ denotes the complex conjugate of F and i the ith path. The vibration power transmission through the ith path can be expressed by using Eqs. (3a)-(3d) as follows:

$$\begin{aligned} P_i(\omega) &= \frac{1}{2}\mathrm{Re}\left\{\bar{F}_i \sum_{j=1}^{6n} Y_{ij}F_j\right\} \\ &= \frac{1}{2}\mathrm{Re}\left\{\left(\sum_{j=1}^{6n} \bar{F}_j \bar{Y}_{ij}\right)F_i\right\} \\ &= \frac{1}{2}\mathrm{Re}\left\{\left(\sum_{j=1}^{6n} \bar{V}_j \bar{Z}_{ij}\right)V_i\right\} \\ &= \frac{1}{2}\mathrm{Re}\left\{\bar{V}_i \sum_{j=1}^{6n} Z_{ij}V_j\right\}. \end{aligned} \tag{5a–d}$$

3. Application to compressor system mounted in outdoor unit of an air conditioner

The outdoor unit of a room air conditioner was chosen to illustrate the practical application of the proposed multi-dimensional vibration power flow approach for vibration/noise reduction. The outdoor unit of an air conditioner shown in Fig. 2 is mainly composed of a compressor, a condenser, a heat exchanger, a fan, a fan motor and a chassis. The compressor is mounted at three points on the base of the chassis and the suction/discharge pipes from the compressor pass through the side panel of the chassis to the indoor unit. It is known that the main sources of the noise from the outdoor unit are the structure-borne noise radiated from the chassis structure and

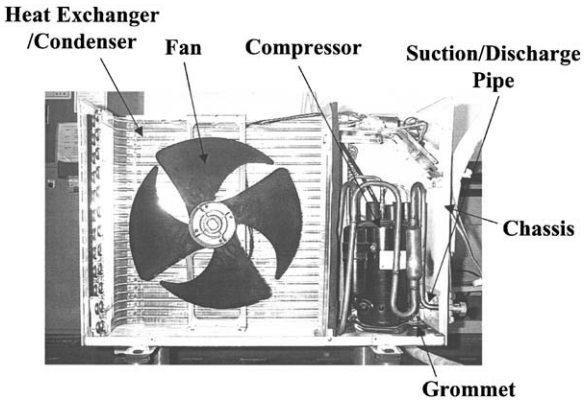

Fig. 2. Outdoor unit of air conditioner.

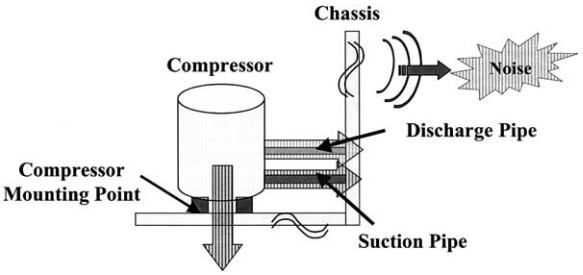

Fig. 3. Major vibration power transmission paths in compressor system mounted in outdoor unit of air conditioner.

airflow noise from the fan. The fan, with an important role in providing heat exchanger and condenser with the airflow, produces the noise mostly at the blade passing frequency and its harmonics, which are relatively in the low frequency range. In this study, we concentrated our focus on the structure-borne sound from the chassis, of which the frequency range is rather high.

Vibration generated in the compressor is transmitted to the chassis structure through several paths and then gives rise to the noise radiation. We first defined several vibration transmission paths and then investigated contribution of each path to the total vibration transmission by employing the vibration power method based on Eqs. (3c) and (5c). The major vibration transmission paths in the compressor system we chose are compressor mounts on the base and suction pipe and discharge pipe on the side panel as shown in Fig. 3.

3.1. Measurement of vibration power flow at connection points between compressor and chassis structure

3.1.1. Selection of measurement points and d.o.f. at each connection point

The compressor is mounted at three points on the base of the chassis, therefore, the total vibration power transmission through the three rubber mounts is the sum of the vibration power transmission through each rubber mount. In this study, only three (one translational and two

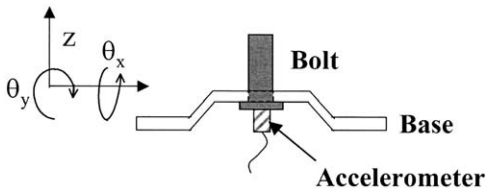

Fig. 4. One translational and two rotational d.o.f.'s for vibration power approximation through each compressor mounting point.

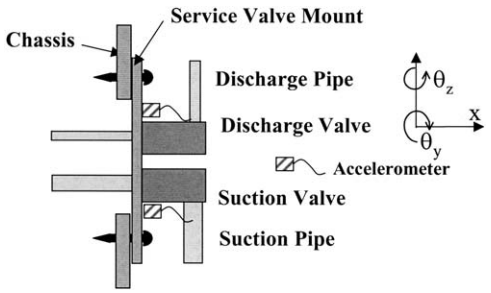

Fig. 5. Vibration power transmission path through service valve mount.

rotational) d.o.f. measurements instead of six d.o.f. were made at each rubber mount as shown in Fig. 4, because the other three d.o.f.'s (x, y, θ_z) are extremely difficult to measure and seem to be less influential in bending wave propagation in thin plate vibrations.

Vibration transmission paths to the chassis through pipes are schematically shown in Fig. 5. Vibration generated from the compressor is transmitted to the suction/discharge valves through the pipes and then, the vibration induced in the valves is transmitted to the chassis through the service valve mount. In measurement of the vibration power flow through each path, first, it needs to determine measurement points near the suction valve and the discharge valve. We could consider three possible measurement points; on the top of the suction/discharge valve, on the service valve mount and on the chassis as shown in Fig. 5. Measurements on the top of the valves can be readily made practically, but make it unreasonable to investigate the effectiveness of isolation of the valves from the service valve mount. Furthermore, measurements on the chassis cannot distinguish the suction pipe path from the discharge pipe path in the vibration power path analysis. Therefore, the measurement points on the service valve mount were selected to estimate the vibration power transmission through the pipes. Three (one translational and two rotational) d.o.f.'s at each of the suction/discharge valves were also considered for the vibration power approximation as shown in Fig. 5.

3.1.2. Approximatation of power flow

As mentioned beforehand, the vibration power transmissions can be approximated preferably based on Eq. (3c), which means that translational and rotational velocities at the connection points of the receiver under operating conditions and the receiver impedance with the compressor disconnected from the chassis are required. In this study, the impedance matrix in Eq. (3c) was obtained by taking inverse of the mobility matrix.

Because three d.o.f.'s at each of the five connection points (including three compressor's rubber mounts) were taken into account, the velocity $\mathbf{V}_R$ in Eq. (3c) becomes a 15×1 vector expressed by

$$\mathbf{V}_R = [V_{1z} \quad V_{2z} \quad V_{3z} \quad V_{sx} \quad V_{dx} \quad \Omega_{1x} \quad \Omega_{2x} \quad \Omega_{3x} \quad \Omega_{sy} \quad \Omega_{dy} \quad \Omega_{1y} \quad \Omega_{2y} \quad \Omega_{3y} \quad \Omega_{sz} \quad \Omega_{dz}]^{\mathrm{T}}, \quad (6)$$

where V and Ω indicate translational velocity and rotational velocity, respectively, and the first subscript, $i = 1, 2, 3$, denotes the compressor's ith rubber mount, s, suction valve and d, discharge valve and the second subscripts, x, y, z, directions of measurements.

Eq. (3c) can be re-expressed by using Eq. (6) and 15×15 impedance matrix of the receiver as follows:

$$P_R = \frac{1}{2}\mathrm{Re}\left\{ [\bar{V}_1, \ldots, \bar{V}_5, \bar{V}_6(=\bar{\Omega}_1), \ldots, \bar{V}_{15}(=\bar{\Omega}_{10})] \begin{bmatrix} \bar{Z}_{(1,1)} & \cdots & \bar{Z}_{(1,15)} \\ \vdots & \ddots & \vdots \\ \bar{Z}_{(15,1)} & \cdots & \bar{Z}_{(15,15)} \end{bmatrix} \begin{bmatrix} V_1 \\ \vdots \\ V_5 \\ V_6(=\Omega_1) \\ \vdots \\ V_{15}(=\Omega_{10}) \end{bmatrix} \right\}. \quad (7)$$

The vibration power transmission to the receiver was estimated based on Eq. (7) which requires cross spectrums between the translational and the rotational velocities at each of the connection points under actual operating condition and the receiver impedance matrix determined by taking the inverse of the mobility matrix.

The cross spectrums of the translational and the rotational velocities were obtained with TAP sensors of Kistler 8832A series which can measure one translational and one rotational accelerations at a given point simultaneously. The cross spectrums between rotational accelerations were determined by installing a single TAP sensor at each connection point in a sequential manner to avoid the mutual effects between two sensors close to each other. That is, $\bar{V}_6 V_{11}(=\bar{\Omega}_{1x}\Omega_{1y})$ was estimated by measuring $\bar{V}_1 V_6(=\bar{V}_{1z}\Omega_{1x})$ and $\bar{V}_1 V_{11}(=\bar{V}_{1z}\Omega_{1y})$ sequentially, each of which can be measured with a single TAP sensor.

Mobility measurement was carried out on the base plate after the compressor was detached from the outdoor unit. The connection points of each path were excited by a mini-shaker over the frequency range 1–1600 Hz. An I-shaped moment arm was used for moment excitation [10] and an impedance head of B&K8001 series for the point mobility measurement.

3.2. Measurement of sound pressure level around and acceleration level on air conditiner outdoor unit

Since the vibration power transmission to the chassis should be closely linked to the overall noise radiation from the chassis, it would be more desirable to measure the sound power level in an anechoic chamber. In this study, however, the space average of the mean-square sound pressure level was simply obtained around the hypothetical surfaces surrounding the source. The spatially averaged acceleration on the vibratory surface of chassis of the outdoor unit was also obtained with the object of comparing with the vibration power flow and sound pressure level.

Fig. 6 shows the sound pressure measurement points on the five surfaces excluding the bottom. The total number of points was 169 ($=42 \times 2$ on each front and rear, $+30 \times 2$ on each right and

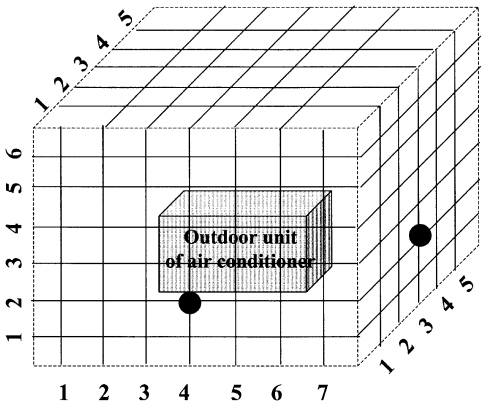

Fig. 6. Sound pressure level measurement points around outdoor unit of air conditioner.

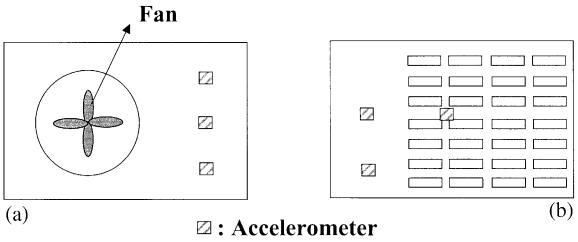

Fig. 7. Acceleration measurement points on outdoor unit of air conditioner: (a) front panel, (b) rear panel.

left, +25 on the top). The distance from the outdoor unit to the measurement surface was taken as 1 m and the distance between the measurement points was 30 cm. The two circles in the figure indicate the position corresponding to the center of the outdoor unit. Fig. 7 shows six acceleration measurement points on the vibratory chassis; three on the front and three on the rear panel.

3.3. Analysis of measurements for current design of compressor system

Although it was found that the noise radiation from the given current design of compressor system was of significance mainly over the frequency range 500–1200 Hz, operational loads on air conditioner compressors may vary significantly depending on the ambient temperature, humidity, operating time and so on and, therefore, lead to inconsistent vibration signals making the steady state analysis inadequate. Since the sound pressure levels and accelerations were measured without employing special equipment such as calorimeter, which can control the ambient temperature and humidity, we first looked into the operational characteristics of the compressor over the frequency range 1–1600 Hz and then chose the frequency range over which those are consistent for further investigation.

Fig. 8 shows six repeated measurements of the total vibration power transmission to the chassis through the rubber mounts, the suction pipe and the discharge pipe. A constant bandwidth of 59 Hz with center frequencies on integer multiples of 59 Hz were used in the spectral analysis

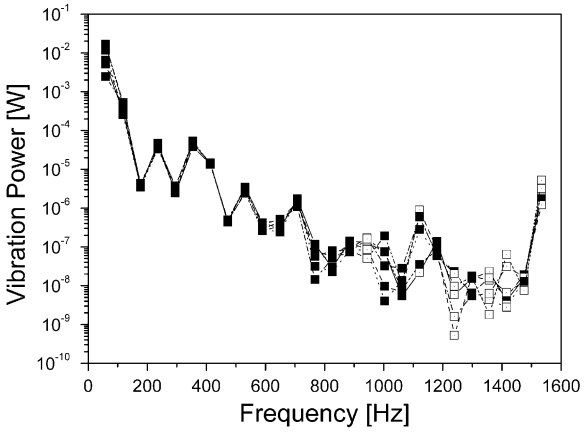

Fig. 8. Repeatability in total vibration power flow measurements: -■-, positive (-□-, negative).

because the vibration spectrum in the preliminary narrow band analysis showed peaks at the harmonics of 59 Hz probably due to the electromagnetic excitations of the motor operating at 59 Hz inside the compressor.

Since the total vibration power transmission to the chassis shows repeatability over the frequency range 100–900 Hz as shown in Fig. 8, it was decided to focus on this frequency range for further vibration power contribution analysis.

The total vibration power transmission to the chassis is the sum of the vibration power transmissions through the three major paths as shown below

$$P = P_M + P_S + P_D, \tag{8}$$

where P_M, P_S and P_D mean the vibration power transmission through the rubber mounts, the suction pipe and the discharge pipe, respectively. The three rubber mounts were treated as a single path in this analysis although they could have been treated as three independent paths by using Eq. (7), because we were concerned about the contribution of the whole mounts in comparison with the other two paths.

To begin with the analysis, we investigated the effects of the rotational vibration power, which is often ignored mainly due to difficulties in instrumentations. When the rotational terms are not measured and/or ignored for simplicity, the 15×1 velocity vector in Eq. (6) reduces to a 5×1 vector:

$$V_{RT} = \begin{bmatrix} V_{1z} & V_{2z} & V_{3z} & V_{sx} & V_{dx} \end{bmatrix}, \tag{9}$$

and, correspondingly, the impedance matrix in Eq. (7) reduces to a 5×5 matrix.

Fig. 9 shows the total vibration power transmissions to the chassis with the rotational terms included and excluded. It can be seen that exclusion of the rotational terms leads to underestimation mainly above 325 Hz. Although the total vibration power flow from the source to the receiver should be positive theoretically, it is not the case in reality. Some negative values were observed at several frequencies as shown in the figure and these are believed to have resulted from some other vibration transmission paths which were not included in the analysis. In

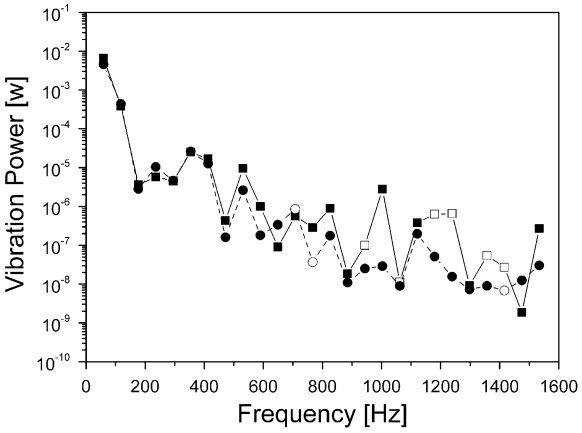

Fig. 9. Total vibration power from compressor to chassis structure through three major paths: rubber mounts, suction pipe and discharge pipe. -■-, With rotational terms included (-□-, negative); -●-, with rotational terms excluded (-○-, negative).

addition, these negative powers may have showed up due to minor experimental errors in the mobility/impedance measurements. For an example, the real parts of the point mobility/impedances and eigenvalues of the mobility/impedance matrix of a linear system should be positive, which is not guaranteed in actual measurement. It has been shown in one of our previous studies that even small measurement errors can be possibly magnified during matrix inversion and distort the power estimation significantly in the forms of faculty peaks of the negative values [11].

It can be also found that the amount of underestimation increases gradually with the frequency. The attachment configuration of the pipes onto the service valve mount seems to be responsible for this phenomenon because the suction/ discharge valves fixed on the service valve mount could play a role of moment arm in the vibration transmission. It can be confirmed by looking into the contribution of the rotational terms in the vibration power transmission through the pipes. Figs. 10 and 11 show the vibration power transmissions from the compressor to the chassis through the rubber mounts and the suction pipe, respectively, with the rotational terms included and excluded. It can be seen in the figures that the amount of underestimation due to exclusion of the rotational terms for the suction pipe path is greater than that of the rubber mounts path above 700 Hz. Therefore, it is confirmed that not only the translational motions but also the rotational motions should be taken into consideration carefully for the vibration power approximations through the pipes especially.

Fig. 12 and Table 1 show the vibration power transmissions through the three major paths: rubber mounts, suction pipe and discharge pipe, where it can be seen that the vibration power was transmitted from the compressor to the chassis dominantly through the discharge pipe over 267–383 Hz, through the rubber mounts over 443–737 Hz, and through the suction pipe over 738–855 Hz. It can be found that the most dominant transmission path varies with the frequency ranges.

Although the total vibration power transmission to the receiver should be positive at all times, the vibration power transmission through a single path/point can be negative in the multi-dimensional vibration isolation system. For example, the direction of vibration power flow

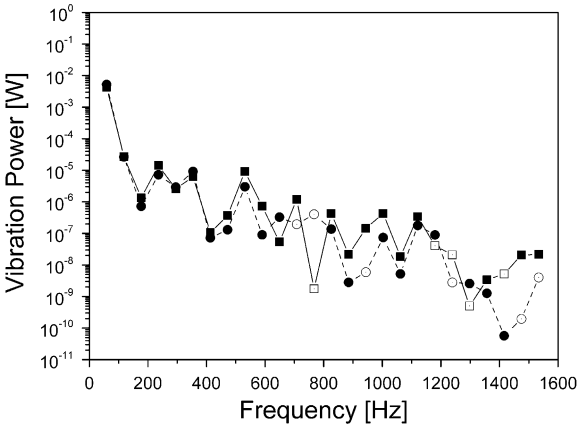

Fig. 10. Vibration power from compressor to chassis structure through rubber mounts. -■-, With rotational terms included (-□-, negative); -●-, with rotational terms excluded (-○-, negative).

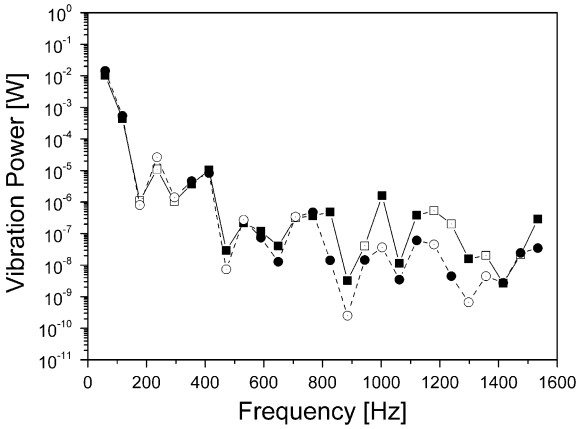

Fig. 11. Vibration power from compressor to chassis structure through suction pipe. -■-, With rotational terms included (-□-, negative); -●-, with rotational terms excluded (-○-, negative).

around 767 Hz can be interpreted in a such way that the vibration power transmitted to the chassis through the suction pipe was predominant over the other paths and some of the vibration power transmitted to the chassis was transmitted back to the compressor through the discharge pipe and rubber mounts.

Fig. 13 shows the spatial distribution of the overall sound pressure level over 100–900 Hz on the front measurement surface of the outdoor unit, where the inner rectangular box indicates the actual size of the front panel of the outdoor unit. The space average of the mean-square sound pressure (overall SPL = 62.8 dB) over the whole hypothetical surfaces surrounding the system has been plotted in Fig. 14 with the total vibration power transmission to and the space averaged acceleration level on the chassis. As could be expected and shown in Fig. 14, the frequency characteristics of vibration power transmitted to the chassis is very closely linked to those of the noise radiation from the chassis. Therefore, it is claimed that the frequency characteristics of noise

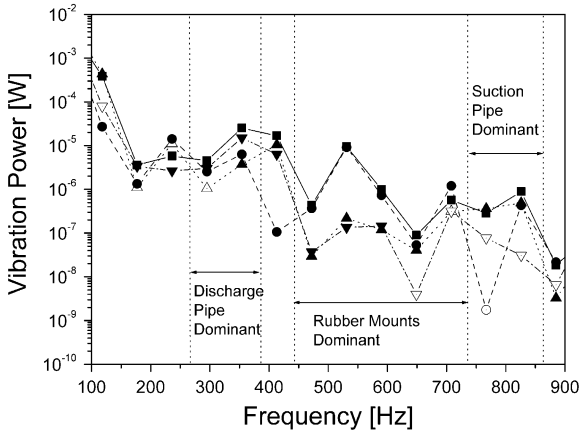

Fig. 12. Vibration power flow from compressor to chassis structure through three major paths: -■-, total vibration power through rubber mounts, suction pipe and discharge pipe; -●-, vibration power through rubber mounts (-○-, negative); -▲-, vibration power through suction pipe (-△-, negative); -▼-, vibration power through discharge pipe (-▽-, negative).

Table 1
Frequency characteristics of vibration power flow via three major paths, sound pressure level and acceleration

Center frequency	Total power ($\times 10^{-6}$ W)	Rubber mounts ($\times 10^{-6}$ W)	Suction pipe ($\times 10^{-6}$ W)	Discharge pipe ($\times 10^{-6}$ W)	SPL (dB)	Acceleration ($\times 10^{-3}$ g^2)
118	380	27	440	−80	58.1	56.5
177	3.6	1.3	−1.1	3.4	53.0	11.8
236	5.8	14	−11	2.7	54.5	50.3
295	4.5	2.5	−1.0	3.0	52.4	33.3
354	25	6.3	3.7	15	55.8	100
413	17	0.11	10	6.3	45.2	13.5
472	0.4	0.37	0.029	0.037	43.9	6.78
531	9.5	9.2	0.22	0.13	47.4	120
590	1.0	0.73	0.12	0.14	45.7	16.5
649	0.1	0.053	0.04	−0.0040	44.0	2.65
708	0.6	1.2	−0.31	−0.32	45.2	6.70
767	0.3	−0.0018	0.36	−0.077	43.4	5.32
826	0.9	0.43	0.49	−0.031	39.9	16.9
885	0.02	0.022	0.0033	−0.0066	40.3	1.92

emission from the outdoor unit can be effectively predicted the vibration power method. It can be also seen that the frequency characteristics of the vibration power transmission to the receiver are similar to those of the accelerations on the receiver. In other words, the noise around the outdoor unit has been built up mostly by the structural vibration of the chassis.

Therefore, it can be concluded that the vibration power can be effectively used to predict qualitively the noise emission from and vibration level on the receiver structure with finite impedance in a vibration isolation system.

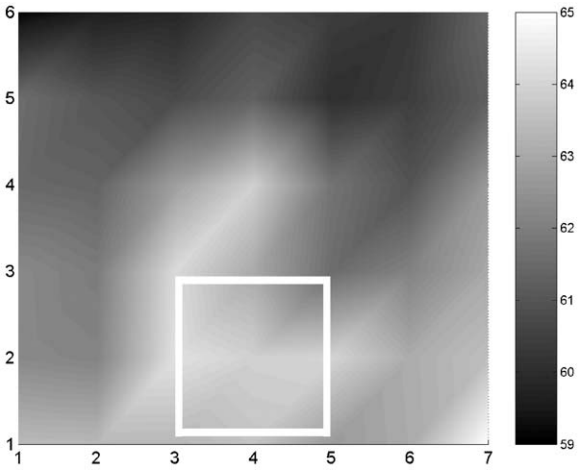

Fig. 13. Spatial distribution of overall sound pressure level (100–900 Hz) on front measurement surface.

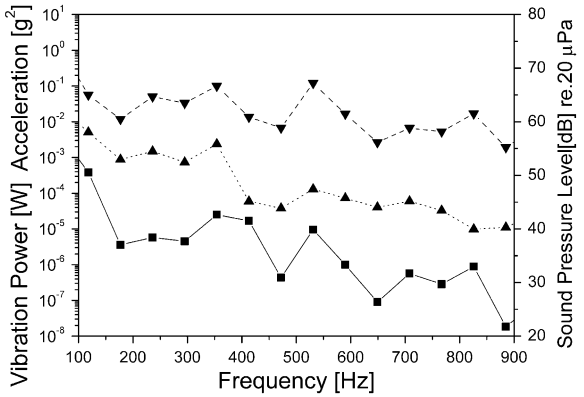

Fig. 14. Comparison of frequency characteristics of: -■-, total vibration power flow from compressor to chassis; -▲-, spatial averaged sound pressure level around; -▼-, acceleration level on; outdoor unit of air conditioner.

3.4. Experimental results for compressor system when suction pipe is isolated from service valve mount

The most dominant vibration power transmission path from the compressor to the chassis was found to be the discharge pipe over 267–383 Hz, the rubber mounts over 443–737 Hz, and the suction pipe over 738–855 Hz as shown in Fig. 12 and mentioned in previous section. For an illustration of the design change and its influence on the vibration power transmission, we isolated one of the three vibration transmission paths, the suction pipe from the service valve mount as shown in Fig. 15 and examined the consequent changes in contribution of each path to the total vibration transmission. The total vibration power flow was compared with the noise radiation from and the structural vibration on the chassis in the same way as in previous section for the

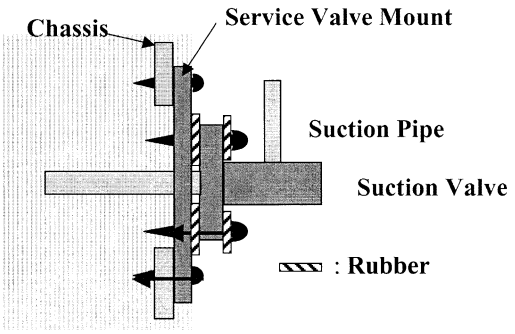

Fig. 15. Isolation of suction valve from service valve mount using rubber-like material.

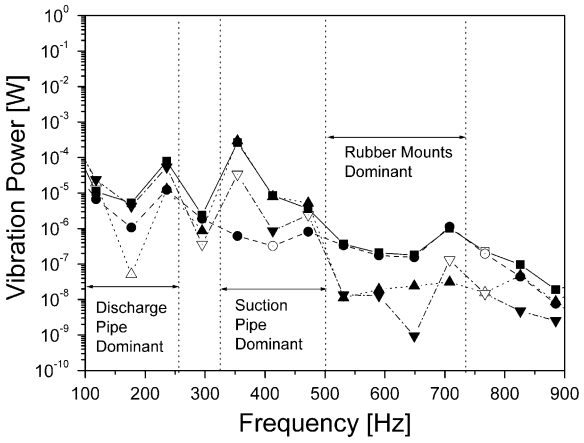

Fig. 16. Vibration power flow from compressor to chassis structure through three major paths when suction valve is isolated. -■-, Total vibration power through rubber mounts, suction pipe and discharge pipe (-□-, negative); -●-, vibration power through rubber mounts (-○-, negative); -▲-, vibration power through suction pipe (-△-, negative); -▼-, vibration power through discharge pipe (-▽-, negative).

purpose of investigating consistency in the frequency characteristics between the vibration power flow and the sound pressure level and how the design modification influences on the noise radiation.

Fig. 16 and Table 2 show the vibration power transmissions when the suction pipe was isolated from the service valve mount, where it can be seen that the contribution of each vibration transmission path has changed with comparison with the case without modifications; the dominant vibration power transmission path was the rubber mounts over 502–737 Hz, the suction pipe over 325–501 Hz and the discharge pipe over 89–265 Hz. It is suspected that the boundary condition changes at the connection point between the suction pipe and the service valve mount gave rise to such a remarkable change in the vibration power flow.

Comparing Fig. 17 with Fig. 13 shows that the isolation of the suction valve resulted in a considerable reduction in sound pressure levels on the front measurement surface of the system.

Table 2
Frequency characteristics of vibration power flow via three major paths, sound pressure level and acceleration when suction pipe is isolated

Center frequency	Total power ($\times 10^{-6}$ W)	Rubber mounts ($\times 10^{-6}$ W)	Suction pipe ($\times 10^{-6}$ W)	Discharge Pipe ($\times 10^{-6}$ W)	SPL (dB)	Acceleration ($\times 10^{-3}$ g^2)
118	11	6.7	−20	24	56.0	42.9
177	5.3	1.1	−0.051	4.2	50.5	2.62
236	79	12	13	54	51.7	57.0
295	2.4	1.9	0.86	−0.36	49.3	45.5
354	260	0.62	300	−34	53.9	846
413	8.5	−0.32	7.9	0.86	46.1	14.6
472	3.6	0.82	5.2	−2.4	43.3	15.3
531	0.36	0.34	0.011	0.013	42.2	1.96
590	0.21	0.17	0.019	0.013	41.1	1.18
649	0.18	0.15	0.024	0.00094	42.2	0.629
708	1.0	1.1	0.031	−0.13	45.5	2.60
767	−0.23	−0.20	−0.016	−0.015	42.8	3.70
826	0.097	0.044	0.048	0.0047	38.8	0.196
885	0.019	0.0076	0.0087	0.0025	37.4	0.114

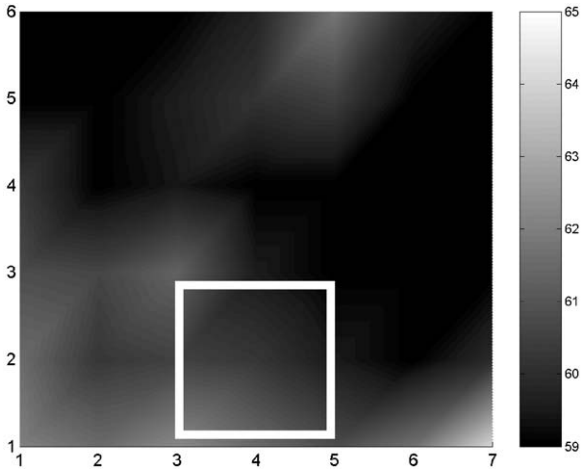

Fig. 17. Spatial distribution of overall sound pressure level (100–900 Hz) on front measurement surface of outdoor unit of air conditioner when suction valve is isolated.

The space average of the mean-square sound pressure (overall SPL = 60.6 dB) over the whole hypothetical surfaces has been plotted in Fig. 18 with the total vibration power flow and the space averaged acceleration level on the chassis in a similar way to Fig. 14. From the analysis of the compressor system, which some modifications were made on, it has been confirmed that the frequency characteristics of the vibration power are very close to those of sound pressure level and acceleration level.

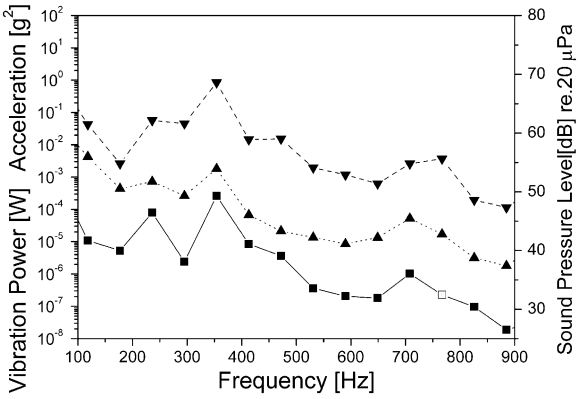

Fig. 18. Comparison of frequency characteristics of: -■-, total vibration power flow from compressor to chassis; -▲-, spatial averaged sound pressure level around; -▼-, acceleration level on; outdoor unit of air conditioner, when suction valve is isolated.

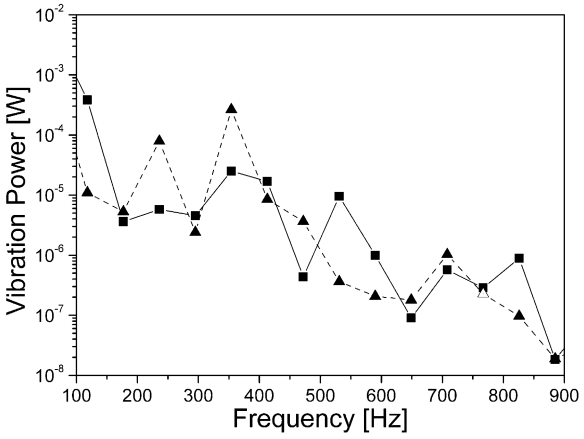

Fig. 19. Comparison of total vibration power flow from compressor to chassis. -■-, Before suction pipe is isolated; -▲-, after suction pipe is isolated (-△-, negative).

Next, we looked into the resultant change in the total vibration power transmission to the chassis, the space average of the sound pressure level induced by, and the acceleration level on, the vibratory surface of the chassis as shown in Figs. 19–21, respectively.

The changes in the frequency characteristics of the vibration power flow caused by inserting an isolator at the suction valve connection point are similar to those of the structural vibration on and the resultant noise emission from the system except at 236 and 354 Hz, where the isolation of the suction valve leads to an increase in the vibration power flow and acceleration level, but a decrease in sound pressure level. The discrepancy is believed to have resulted from the fan noise whose fundamental blade passing frequency is 42 Hz (625 r.p.m., four blades) and the structural-borne noise induced in the suction and discharge pipe, which was ignored in this study, because the changes in frequency characteristics of the vibration power are similar to the one of the acceleration level.

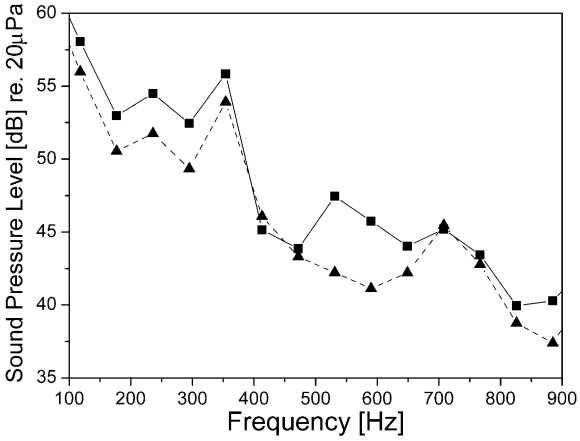

Fig. 20. Comparison of spatial averaged sound pressure level around chassis. -■-, Before suction pipe is isolated; -▲-, after suction pipe is isolated.

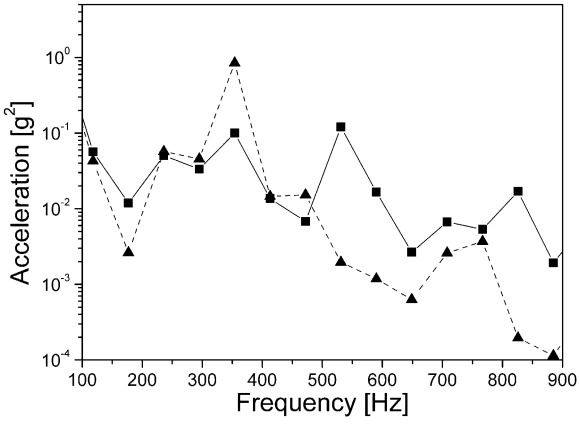

Fig. 21. Comparison of averaged acceleration level on chassis. -■-, Before suction pipe is isolated; -▲-, after suction pipe is isolated.

4. Conclusions

The concept of vibration power was to be applied to a compressor system mounted in outdoor unit of an air conditioner for the vibration transmission path analysis. For that purpose, we estimated the vibration power transmission from the compressor to the chassis through three major paths: the rubber mounts, the suction pipe and the discharge pipe and then investigated the contribution of each path to the total vibration power transmission. Furthermore, three (one translational and two rotational)-d.o.f. vibrations at each connection point were measured in order to look into the effects of neglecting the rotational terms on the total vibration power estimation. In addition, the structural vibrations of the chassis and sound radiation from it were also measured and compared with the total vibration power transmission.

Experimental results show that the vibration power approximation with the rotational terms ignored can be underestimated especially over a high-frequency range. As can be expected, it is shown that the hard connections such as the pipes are more contributing to the transmission of the rotational vibration power than the soft connections such as rubber mounts.

The vibration power path analysis on the compressor illustrates the most dominant transmission path out of the several candidates at each specific bandwidth of frequencies. It is also shown that the vibration power approach is effective in describing the direction of the energy flow in each path and representing the contribution of each path to the total vibration transmission in a simple way.

It has been shown that the frequency characteristics of the vibration power flow are very similar to those of the sound pressure level around and the acceleration level on the vibratory surface of the outdoor unit of the air-conditioner. Therefore, it is concluded that the vibration power can be effectively used to predict qualitively the vibration level on and the noise radiation from the receiver structure in a vibration isolation system. That is, when changes in the design variables such as geometrical shapes and material properties of a subsystem; the source, the isolators and the receiver, are to be made, the vibration power approach will be able to predict the frequency characteristic of the noise radiation from the receiver structure because the vibration power transmission can be estimated by using the dynamic characteristics of the subsystems [9].

Acknowledgements

This work has been financially supported by KOSEF (Korea Science and Engineering Foundation: 98-0200-06-01-3) during 1998–2001.

References

[1] A.T. Moorhouse, B.M. Gibbs, Measurement of structure-borne sound emission from resiliently mounted machines in situ, *Journal of Sound Vibration* 180 (1995) 143–161.

[2] B.M. Gibbs, A.T. Moorhouse, Case studies of machine bases as structure-borne sound sources in buildings, *International Journal of Acoustics and Vibration* 4 (3) (1999) 125–133.

[3] Y.K. Koh, R.G. White, Analysis and control of vibrational power transmission to machinery supporting structures subjected to a multi-excitation system, part II: vibrational power analysis and control schemes, *Journal of Sound and Vibration* 196 (1996) 495–508.

[4] Y.K. Koh, R.G. White, Analysis and control of vibrational power transmission to machinery supporting structures subjected to a multi-excitation system, part III: vibrational power cancellation and control experiments, *Journal of Sound and Vibration* 196 (1996) 509–522.

[5] P. Gardonio, S.J. Elliott, R.J. Pinnington, Active isolation of structural vibration on a multiple-degree-freedom system, part I: the dynamics of the system, *Journal of Sound and Vibration* 207 (1997) 61–93.

[6] P. Gardonio, S.J. Elliott, R.J. Pinnington, Active isolation of structural vibration on a multiple-degree-freedom system, part II: effectiveness of active control strategies, *Journal of Sound and Vibration* 207 (1997) 95–121.

[7] C.Q. Howard, S.D. Snyder, C.H. Hansen, Calculation of vibratory power transmission for use in active vibration control, *Journal of Sound and Vibration* 233 (2000) 573–585.

[8] M.A. Sanderson, Vibration isolation: moments and rotations included, *Journal of Sound and Vibration* 198 (1996) 171–191.

[9] H.-J. Lee, K.-J. Kim, A study of the effects of rotational terms in the power transmission through vibration isolation systems on beam-like structures, *International Journal of Acoustics and Vibration* 5 (3) (2000) 127–134.
[10] M.A. Sanderson, Direct measurement of moment mobility, part II: an experimental study, *Journal of Sound and Vibration* 179 (1995) 685–696.
[11] H.-J. Lee, K.-J. Kim, Qualification of mobility matrix in multi-dimensional vibration power path analysis, *Sixth Biennial Conference on Engineering Systems Design and Analysis*, Istanbul, Turkey, ESDA2002/APM-020, 2002.